RSC Advances

PAPER

View Article Online
View Journal | View Issue

Cite this: *RSC Adv.*, 2026, **16**, 1888

Ultra-sensitive low-frequency dual-mode humidity sensor using a methyl red-PVA-graphene oxide composite

Mushahid Hussain, †*[ab] Nadir Ali Khan,[a] Wei-Chun Lin,[b] Muhammad Yaseen, [c] Fakhra Aziz,[a] Muhammad Ali[d] and Naseem Abbas†[e]

In this study, a novel ternary composite (MPG), composed of methyl red (MR), polyvinyl alcohol (PVA), and graphene oxide (GO), is synthesized and employed for the fabrication of a humidity sensor. To explore its potential for humidity sensing applications, the structural and morphological characteristics of the MPG composite were analyzed using SEM, XRD, FTIR, and UV-visible spectroscopy. The composite demonstrated a well-integrated, crosslinked microstructure enriched with functional groups and carbon-based elements, which are highly conducive to water molecule adsorption. A 678 nm thick MPG film was deposited onto an interdigitated electrode *via* spin coating, followed by thermal annealing at 100 °C. The sensor exhibited stable and reliable performance across a wide humidity range (32–92% RH) at 25 °C, featuring a high capacitive sensitivity of 11 nF/%RH at 100 Hz, rapid response and recovery times of 6 and 8 seconds, respectively, and a low hysteresis of 17.3%. Additionally, the electrical performance of the MPG composite film was evaluated over a voltage range of −5 to 5 V at various temperatures. Results revealed enhanced conductivity with increasing temperature, attributed to increased lattice vibrations and the generation of thermally activated charge carriers. This temperature-dependent behavior highlights the composite's suitability for use in electronic devices that operate under diverse thermal conditions. This cost-effective ternary composite-based humidity sensor shows promise for use in hygrometers and real-time relative humidity monitoring in electronic devices.

Received 30th September 2025
Accepted 23rd December 2025

DOI: 10.1039/d5ra07420g

rsc.li/rsc-advances

1 Introduction

Humidity sensors are vital for various applications, including industrial, agricultural, and medical fields, due to their ability to measure ambient moisture levels.[1–3] These sensors are integral to various fields, including industrial processing, meteorology, environmental control, pharmaceuticals, agriculture, and domestic climate control. Considerable research has been conducted to improve the response/recovery times, as well as the long-term stability, of humidity sensors by investigating novel materials and device architectures.

Organic materials have attracted attention due to their broad sensing range, linear response, rapid response and recovery, low hysteresis, and cost-effectiveness. The selection of sensing material is paramount, as the interaction between water vapor and the sensor surface induces variations in electrical resistance and capacitance, necessitating the exploration of new materials and structures. Researchers are focusing on organic materials due to their broad sensing range, linearity, short response and recovery times, low hysteresis, and cost-effectiveness. The choice of material is crucial, as the interaction of water vapors with the sensor surface leads to changes in resistance and capacitance.[4–8] A wide range of composites, including polymers and carbon-based derivatives with tunable properties and facile synthesis, have emerged as promising candidates for advanced humidity sensors.[8–10]

Polymers have gained prominence in sensor fabrication owing to their mechanical flexibility and advantageous physicochemical properties. Among these, poly(vinyl alcohol) (PVA), a water-soluble polymer, is particularly favored for its hydrophilicity, high chemical resistance, and thermal stability.[11,12] However, pure PVA exhibits intrinsically high resistance, which compromises its sensitivity and response time when used alone.[13] Incorporating conductive materials into PVA matrices effectively lowers their resistance and markedly improves sensitivity.[14] For example, embedding PVA into a polyaniline (PANI) matrix results in notable changes in resistance, enhancing humidity responsiveness.[15] Generally, the addition

[a]*Department of Electronics, University of Peshawar, Peshawar, 25120, Pakistan. E-mail: mushahidhussain708@gmail.com*

[b]*Department of Photonics, National Sun Yat-sen University, No. 70, Lianhai Rd., Gushan Dist., Kaohsiung, Taiwan, Republic of China*

[c]*Department of Chemistry, Division of Science & Technology, University of Education, Lahore, Pakistan*

[d]*Department of Physics, University of Peshawar, Peshawar, 25120, Pakistan*

[e]*Department of Mechanical Engineering, Sejong University, Seoul, 05006, Republic of Korea*

† Authors are equally contributed to this work.

of conductive fillers to PVA forms composites with reduced resistance and improved performance.[16,17]

Graphene and its derivatives—particularly graphene oxide (GO)—have been extensively explored due to their exceptional physicochemical characteristics.[18] GO is especially appealing because of its amphiphilic structure and abundant oxygen-containing functional groups (*e.g.*, hydroxyl and carboxyl), which promote hydrogen bonding and dispersibility in aqueous or polar solvents[19]{Banerjee, 2018 #374}. Its hydrophilicity, electrical conductivity, high porosity, and extensive surface area make GO a highly effective moisture adsorbent, facilitating the adsorption and penetration of water molecules and pollutants into its layered structure. GO has been successfully integrated into capacitive humidity sensors.[20]

Zubair *et al.* demonstrated that MR reduces electrical resistance upon moisture exposure, suggesting its suitability for capacitive humidity sensing.[21] Ali *et al.* developed a highly sensitive humidity sensor by integrating graphene with MR, capitalizing on graphene's wide sensing range and MR's selectivity against cross-sensitivity from interfering air components.[10,22] MR offers dual functionality: it absorbs water molecules, thereby reducing film resistance, and fills voids between graphene flakes, enhancing film uniformity and overall sensor performance.[10]

Hassan *et al.* reported a humidity sensor based on individual spin-coated layers of PEDOT: PSS, MR, and GO on separate interdigitated electrodes, electronically connected in series to achieve full-range humidity sensing.[23] In contrast, the present work utilizes a ternary composite of MR, PVA, and GO, spin-coated onto a single interdigitated electrode in a simplified fabrication process. This composite is designed to leverage the synergistic properties of its constituents: PVA offers high water adsorption capacity but suffers from high resistance, which is mitigated by the excellent electrical conductivity of GO. However, GO's sensitivity to multiple gases necessitates improved selectivity, which is addressed by incorporating MR. MR functions to suppress GO's cross-sensitivity and improve overall sensor accuracy.[22,24,25]

Thin-film-based resistive and capacitive sensors are recognized for their low power consumption, enhanced sensitivity and selectivity, superior stability, and fast response/recovery characteristics.[26,27] Therefore, this study aims to develop and evaluate a thin-film sensor based on the MR-PVA-GO ternary system for potential humidity-sensing applications.

2 Experimental section

2.1 Materials

Methyl red (MR), with a molecular formula of $C_{15}H_{15}N_3O_2$, a molecular weight of 269.31 g mol^{-1}, and a melting point between 179–182 °C, Assay 95%, was purchased from British Drug Houses (BDH) Chemicals, England. Polyvinyl alcohol (PVA), with a molecular weight of 10 000 g mol^{-1} and a melting point between 180–190 °C, with an Assay of 99.8%, was purchased from Sigma Aldrich. Graphite powder with a molecular weight of 12.01 g $mole^{-1}$, Assay 98.5%, was purchased from AVONCHEM, Limited. All chemicals, including distilled water (H_2O), ethanol (C_2H_6O), dimethyl sulfoxide [$(CH_3)_2SO$], hydrochloric acid (HCl), and sulfuric acid (H_2SO_4), were obtained from Sigma-Aldrich. Sodium nitrate ($NaNO_3$), potassium permanganate ($KMnO_4$), and hydrogen peroxide (H_2O_2) were provided by Merck Group, Germany. The solutions were prepared using weight-to-weight (w/w) or weight-to-volume (w/v) percent.

2.2 Synthesis of graphene oxide

Graphene oxide (GO) was synthesized using a modified Hummers' method.[28] In a typical procedure, 3.0 g of graphite powder and 2.0 g of sodium nitrate were added gradually to 100 mL of concentrated sulfuric acid in a round-bottom flask, maintained at 5 °C, under continuous stirring. After 30 minutes of mixing at this temperature, 10 g of potassium permanganate was added slowly while maintaining stirring for an additional 24 hours at room temperature, with continuous oxygen bubbling to enhance the oxidation process.

Subsequently, the reaction mixture was subjected to reflux for another 24 hours. After cooling, 50 mL of 3% hydrogen peroxide (H_2O_2) was added, leading to a color change from dark brown to bright yellow, indicating successful oxidation of graphite into graphite oxide. The product was filtered and thoroughly washed with 5% hydrochloric acid to eliminate residual ions and impurities. The washed material was dried in an oven, followed by purification *via* centrifugation at 3000 rpm for 30 minutes. Finally, graphite oxide was exfoliated into GO nanosheets using a standard ultrasonication-based exfoliation technique.[29]

2.3 Preparation of MPG composite

A polyvinyl alcohol (PVA) solution was prepared by dissolving 2.0 g of PVA in a binary solvent system consisting of 50 mL deionized water and 50 mL ethanol. The solution was stirred at room temperature until complete dissolution was achieved. Subsequently, 2.0 g of methyl red (MR) was added to the PVA solution and stirred thoroughly to form a homogeneous blend.

In parallel, a graphene oxide (GO) dispersion was prepared by dispersing 0.4 g of GO in 20 mL of dimethyl sulfoxide (DMSO). This dispersion was stirred continuously for 24 hours at ambient temperature to ensure uniform dispersion of GO in the DMSO medium. Afterward, 2.0 g of the previously prepared MR-PVA mixture was added to the GO dispersion, and the entire mixture was stirred until a uniform ternary composite comprising methyl red, polyvinyl alcohol, and graphene oxide (MPG) was obtained. The MPG mixture was then subjected to slow evaporation at room temperature, yielding a solid MPG composite. The schematic representation of the composite is presented in Fig. 1(a).

2.4 Fabrication of MPG humidity sensor

An interdigitated alumina electrode (IDE) was employed as the substrate for sensor fabrication. The cross-sectional structure of the IDE is shown in Fig. 1(c), where the bottom conductive layer is composed of silver (Ag), the electrode body is made of alumina (Al_2O_3), and the top layer consists of the deposited

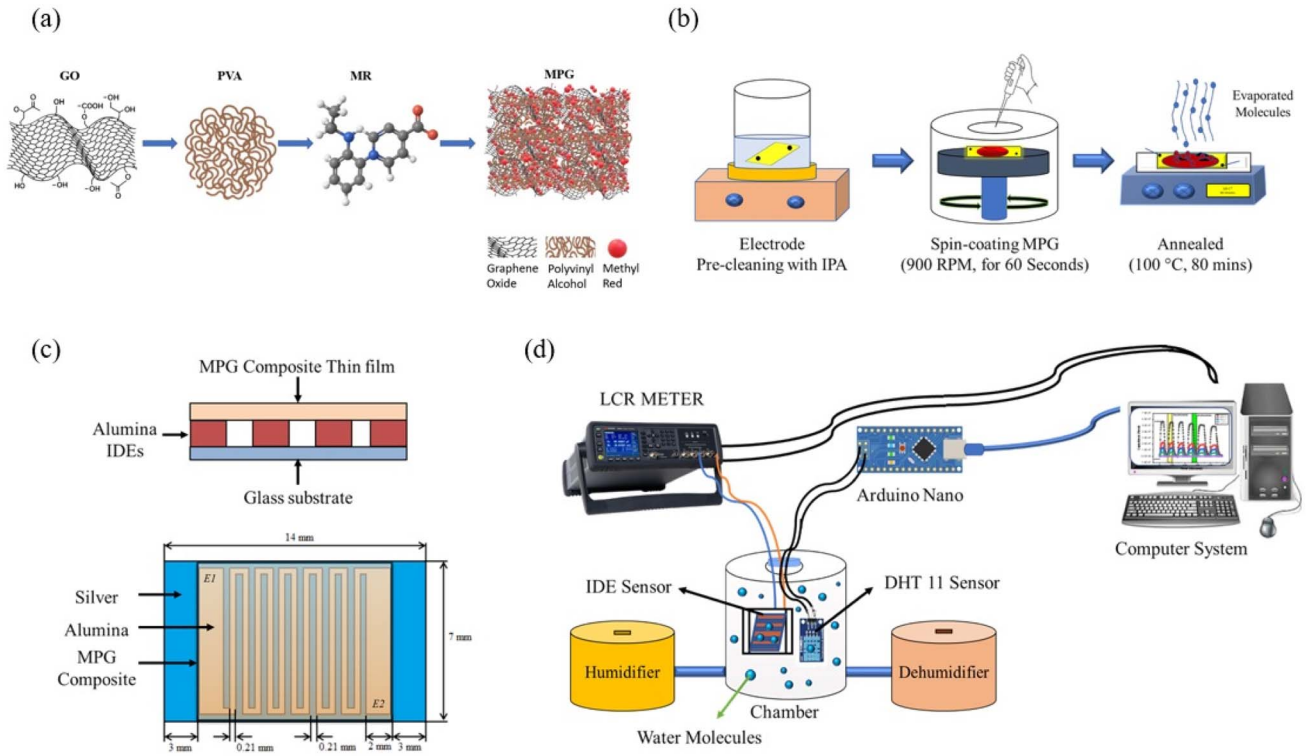

Fig. 1 (a) Schematic flow chart for the preparation of the MPG composite, along with its chemical structure, (b) step by step illustration of the IDE cleaning and MPG device fabrication process, (c) side and top views of the Interdigitated Electrode (IDE) based humidity sensor, showing device dimensions and schematic layout, and (d) schematic diagram of the self-made humidity set-up for measuring capacitive and resistive response against relative humidity.

sensing material. The IDE dimensions measure 14 × 7 mm^2 (total area: 98 mm^2), with both line width and line spacing set at 0.21 mm, as illustrated in Fig. 1(c). A simplified top-view schematic of the MPG composite-based resistive-type humidity sensor[30] is also provided in the actual Fig. S4.

The film thickness of the deposited MPG was controlled through optimized spin-coating parameters (0.5 μL volume at 900 rpm for 60 seconds), resulting in a film of 678 nm thickness, as evaluated using a stylus profilometer (Dektak), which confirmed uniform thin-film deposition. The deposition was performed using a Laurell WS-650 spin coater (Laurell Technologies, USA). The IDE electrode was affixed to a glass slide using adhesive tape, and a masking layer was applied to define the deposition area, ensuring selective coating of the active electrode region only.

Prior to film deposition, the IDE substrate was thoroughly cleaned by sequential rinsing with ethanol and deionized water. It was then placed in an ultrasonic cleaner for 20 minutes to remove residual surface contaminants, as depicted in Step 1 of Fig. 1(b). After cleaning, the substrate was dried under ultraviolet (UV) light exposure to ensure complete removal of moisture.

The device was fabricated *via* a simple spin-coating method, following the procedure illustrated in step 2 of Fig. 1(b). A 0.5 μL aliquot of the MPG composite was dispensed onto the IDE surface using a Nichipet Premium Lt. pipette, and spin-coated at 900 rpm for 60 seconds to yield a uniform, homogeneous thin film.

Subsequently, the deposited MPG film was annealed at 100 °C for 80 minutes to enhance its structural, electrical, and sensing properties, as shown in Step 3 of Fig. 1(b). After annealing, the sample was allowed to cool naturally to room temperature. The annealing process is expected to reduce intrinsic defects, improve film crystallinity, and enhance charge transport pathways within the MPG composite matrix.[31]

2.5 Characterization and measurements

The surface morphology of the MPG composite thin films was examined using Scanning Electron Microscopy (SEM) on a JEOL JSM-IT100 microscope (Japan). Elemental analysis of the film was performed *via* Energy-Dispersive X-ray Spectroscopy (EDS) using an SEM system equipped with an integrated energy-dispersive X-ray detector. X-ray diffraction (XRD) patterns of the MPG powder were recorded using a JEOL JDX-3532 X-ray diffractometer (Japan), employing CuKα radiation ($\lambda = 1.5418$ Å) to analyze the crystallographic structure Fig. S5.

Fourier-transform infrared (FTIR) spectra of the neat GO, PVA, MR, and ternary composite MPG were recorded in the wavenumber range of 4000–450 cm^{-1}, with a spectral resolution of 0.1 cm^{-1} and 25 scans per sample, using an Agilent Technologies Cary 630 FTIR spectrometer (Santa Clara, CA, USA) equipped with a DLaTGS (deuterated L-alanine doped triglycine sulfate) detector Fig. S6. UV-Vis absorption spectra in the 200–800 nm range were obtained at normal light incidence and

room temperature, with a wavelength interval of 0.1 nm, using a Shimadzu UV-3150 UV–VIS–NIR spectrophotometer Fig. S6.

The electrical properties of the MPG thin film were measured using a Keithley 4200 semiconductor characterization system. Humidity-dependent resistance and capacitance responses were evaluated in a custom-designed humidity chamber, illustrated in Fig. 1(d). During measurements, the humidity sensor was positioned inside the chamber, and the relative humidity (RH) was monitored using a DHT-11 sensor interfaced with an Arduino Nano microcontroller, which transmitted data to a computer for real-time humidity display.

Sensor electrodes were connected to an Agilent E4980A precision LCR meter (operating from 20 Hz to 2 MHz) to acquire resistance and capacitance data. Humidity inside the chamber was regulated using a humidifier and dehumidifier, allowing control of RH to observe the adsorption and desorption behavior of the composite sensor. The humidifier increased the RH beyond 75%, simulating a mist-laden environment. LabVIEW software was used for automated data acquisition. All measurements were conducted at fixed temperature of 25 °C (±0.01 °C), with RH incremented in 5% steps over a range of 32–92%.

3 Results and discussion

3.1 Design rationale

The MPG composite, composed of methyl red (MR), polyvinyl alcohol (PVA), and graphene oxide (GO), has been strategically designed to exploit the synergistic functionalities of its constituents for humidity sensing applications. This novel ternary system represents the first reported use of this specific combination in a humidity sensor, fabricated *via* a facile and scalable solution-based method. Each component plays a distinct but complementary role in enhancing the overall performance of the sensor. PVA, a hydrophilic polymer known for its excellent film-forming ability and water affinity, serves as the primary moisture-sensitive matrix.[32] Its abundant hydroxyl groups enable efficient adsorption of water molecules from the surrounding environment, thereby significantly increasing the composite's humidity sensitivity. However, PVA alone suffers from poor electrical conductivity,[33] which limits its direct application in electronic sensing devices.

To overcome this limitation, graphene oxide is incorporated into the matrix. GO possesses a high specific surface area, layered porosity, and oxygenated functional groups that not only facilitate additional moisture adsorption but also significantly enhance the electrical conductivity of the composite. This compensates for the intrinsic resistive nature of PVA, enabling a more responsive electrical signal during humidity detection. Furthermore, GO promotes uniform dispersion of both MR and PVA due to its excellent compatibility with polar solvents such as water, ethanol, and DMSO, which are crucial for thin-film fabrication processes.

Methyl red is added as a functional dye with favorable electronic and optical properties. Although it is relatively rigid in structure, MR contributes to the humidity sensing behavior through subtle structural changes under varying environmental conditions.[34] Its conjugated π-electron system allows interaction with GO *via* π–π stacking, facilitating charge transfer processes and potentially enhancing the sensor's sensitivity and response time. The presence of MR in the composite also facilitates the achievement of a more homogeneous film morphology, thereby contributing to improved reproducibility and stability in sensor performance.

Altogether, the MPG composite combines the high water adsorption capacity of PVA, the electrical conductivity and structural support of GO, and the functional responsiveness of MR. These synergistic interactions result in a stable, low-cost, and solution-processable material that forms uniform thin films with excellent humidity sensitivity. The commercial availability and low toxicity of all three components further underscore the practicality and scalability of this composite for real-world sensing applications, particularly in the development of flexible, low-cost humidity sensors.

3.2 Characterization

3.2.1 Scanning electron microscopy. Typically, scanning electron microscopy (SEM) provides information on the uniformity of the composite, the presence of voids, and the existence of aggregates. Fig. 2(a–c) shows SEM micrographs of the ternary composite thin film comprising PVA, MR, and GO after being annealed at 100 °C for 80 minutes. The surface morphologies of pristine MR, GO and PVA thin film are presented in SI (Fig. S1). The surface morphology of pristine polyvinyl alcohol micrographs exhibits a polymeric texture means semicyrstalline structure Fig. S1(a and b), whereas pristine MR micrographs Fig. S1(c and d) shows irregular particle-like aggregates. However, pristine GO micrographs Fig. S1(e and f) displays a highly porous structure. The surface morphologies of pristine MR and GO thin films, as reported in (ref. 23), revealed defect-free films with no visible cracks. However, the GO thin film showed a highly porous surface, suggesting a high surface area-to-volume ratio. On the other hand, PVA exhibits magnificent film-forming properties and acts as a host matrix and binder due to its hydrophilic nature. In the MPG thin film, PVA supports a stable integration of MR and GO, ensuring uniform dispersion and adhesion. Fig. 2(b and c) illustrates the homogeneous dispersion of the composite matrix, attributed to the presence of hydroxyl groups in PVA. A crosslinked polymer microstructure with enhanced porosity and a high surface area-to-volume ratio, attributed to the inclusion of GO, is demonstrated in Fig. 2. These features are advantageous for optimal water molecule adsorption and improved hydrogen molecule adsorption, along with increased capacitance. The MPG thin film also exhibits increased surface roughness due to the incorporation of GO. This enhanced roughness is anticipated to improve the film's sensing performance by facilitating better interaction with water molecules, resulting in faster response/recovery times, as well as higher sensitivity. Fig. 2(a) also indicates that there are no cracks on the electrode surfaces, suggesting improved ion mobility.

The elemental composition was analyzed by EDX mapping, with the data for the annealed MPG film presented in Fig. 2(d–

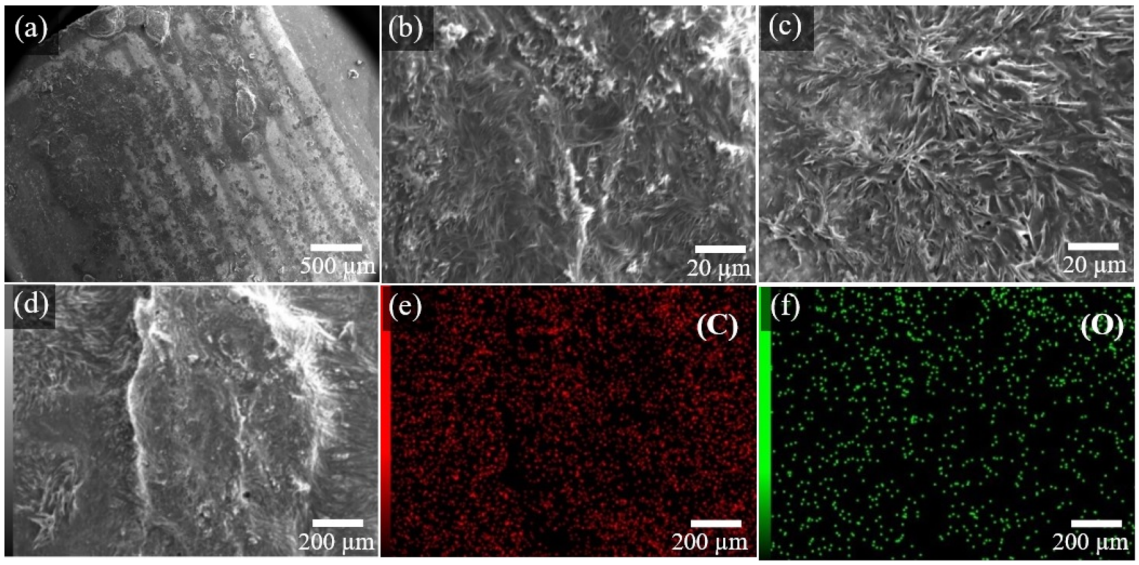

Fig. 2 SEM micrographs, (a) annealed MPG thin film at 500 μm, (b) annealed MPG thin film an electrode at 20 μm, (c) an electrode at 20 μm, and (d)–(f) elemental mapping of MPG thin film at 200 μm, (e) carbon, (f) oxygen.

f). The EDX spectra and mapping confirm the presence of carbon (70.33%), and oxygen (29.67%), in the composite. The existence of the three moieties in the MPG thin film is verified through EDX analysis, which highlights the main content of C and O elements in the composite nanofibers. These findings corroborate the enhanced structural and compositional properties of the annealed MPG composite, making it suitable for effective humidity sensing applications.

3.3 Humidity sensing properties

Fig. 3 presents resistance/capacitance *versus* relative humidity variations and sensitivities of the MPG composite-based humidity sensor at various operating frequencies *i.e.*, 100 Hz, 300 Hz, 500 Hz, 1 kHz, and 10 kHz over a constant voltage of 1 V, at 25 °C. Fig. 3(a) shows a decrease in the sensor's resistance with increasing relative humidity. The plot indicates that the resistance of the MPG humidity sensor decreases while the conductivity of the sensor increases with increasing relative humidity for all operating frequencies. At 100 Hz, the resistance of the sensor decreases linearly, exhibiting a sharp decrease with rising humidity up to 85% RH, and then saturates. However, at higher frequencies, the sensor's response becomes less linear and decreases gradually. A notable deviation is observed at 500 Hz, where the sensor's resistance increases above 60% relative humidity (RH). This behavior can be attributed to resonance effects within the sensing material. At this frequency, dipolar polarization of water molecules and charge trapping predominate, disrupting the ionic conduction pathway and resulting in higher resistance.[35] The resistive response of the sensor was calculated using the following mathematical eqn (1).[36]

$$R = \frac{R_{32} - R_{85}}{85 - 32} \quad (1)$$

R_{85} is the sensor's resistance at 85% RH, beyond which the resistance of the sensor becomes constant and independent of the relative humidity. R_{32} is the sensor's resistance at 32% RH, the lowest relative humidity. The response of the sensor was measured at five different frequencies, *i.e.*, 100 Hz, 300 Hz, 500 Hz, 1 kHz, and 10 kHz, as shown in Fig. 3(c). The sensor exhibited its best sensitivity towards resistive type (∼135.8 Ω/% RH) at 100 Hz, with sensitivities of 112.55 Ω/%RH, 101.42 Ω/% RH, 93.72 Ω/%RH, and 83.49 Ω/%RH at frequencies of 300 Hz, 500 Hz, 1 kHz, and 10 kHz, respectively.

Fig. 3(b) illustrates the variation in capacitance of the sensor with increasing relative humidity. The response curves in the figure demonstrate that the capacitance of the MPG humidity sensor increases with increasing relative humidity for all operating frequencies within the humidity range of 32–92 %RH. From Fig. 3(b), it can also be observed that the capacitance change directly depends on the operating frequencies. Moreover, the device responds well at lower frequencies as compared to higher frequencies. As the frequency increases, an increase in the capacitance becomes less conspicuous and consequently shows little dependence on %RH. Thus, it may be speculated that the ionic polarization is unable to keep up with changes in the electric field at high frequencies, therefore making capacitance less dependent on relative humidity.[37] The sensitivity of a sensor is defined as a change in capacitance per degree rise in relative humidity. The sensitivity of a humidity sensor is calculated using the following mathematical eqn (2).

$$S = \frac{C_{92} - C_{32}}{92 - 32} \quad (2)$$

The 32% RH is the lowest relative humidity at which capacitance begins to increase, and 92% RH is the highest relative humidity at which the most significant value of capacitance is obtained; C_{32} and C_{92} are the capacitances at 32% and

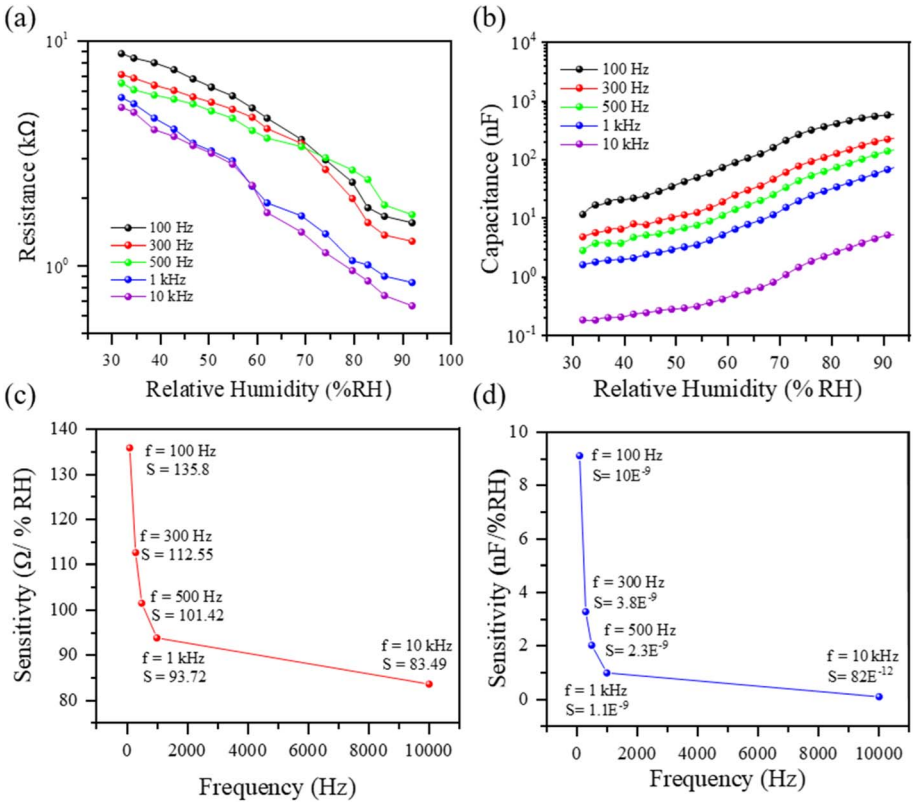

Fig. 3 (a) Resistance, and (b) capacitance *versus* relative humidity response of MPG composite-based sensor at five different frequencies, at 25 °C; sensitivity *versus* (c) resistance and (d) capacitance of the humidity sensor.

92% RH, respectively. The sensitivity of the fabricated sensor is measured at all five frequencies, *i.e.*, 100 Hz, 300 Hz, 500 Hz, 1 kHz, and 10 kHz, as shown in Fig. 3(d). The sensitivity was found to be 11 nF at 100 Hz, 3.8 nF at 300 Hz, and 2.3 nF at 500 Hz. The sensitivity further decreased for higher frequencies and was obtained as 1.2 nF and 83 pF at 1 and 10 kHz, respectively; this demonstrated that the sensor sensitivity continues to decrease with increasing frequency.

It can be observed from Fig. 3(b) that the sensor is more sensitive at low frequencies compared to higher frequencies. The operating frequency controls the orientation of the polar water molecule adsorbed by the sensor. The frequency orients and reorients water molecules, which in turn affect the polarization of the active material. At lower frequencies, water molecules can easily follow the operating frequency. However, at higher frequencies, it becomes difficult for water molecules to follow the rapidly changing electric field due to the inertia of the molecules, which ultimately leads to low sensitivity.[38] Since inertia depends on molecular size, larger molecules tend to have more inertia than smaller molecules.

It can also be inferred that the device's highest sensitivity is achieved at a frequency equal to or lower than 100 Hz at 1 V (rms). However, it must be underlined that although the sensitivity of the humidity sensor at frequencies below 100 Hz would still be higher, the stability and repeatability of the sensor would be considerably compromised. Such behavior has been observed by Zhang *et al.*, who reported an unsteady humidity response at 40 Hz.[39] Similarly, multi-walled carbon nanotubes incorporated humidity sensors, when investigated at 50 Hz, also demonstrated adverse effects on stability and repeatability.[40] Hence, it is advisable to avoid electrical characterization of the humidity sensor below 100 Hz.[41]

The fabricated MPG humidity sensor was placed in a controlled humidity chamber for analysis of response and recovery. Fig. 4(a and b) show the response and recovery behavior of the co-planar MPG humidity sensor. The response time is determined by rapidly inserting the sensor into a continuous humidified environment from 32–92% RH. It is the time consumed by the sensor to reach 90% of its final relative humidity value. However, recovery time is measured when the sensor is placed inside the chamber under continuous desiccation from 92–32% RH. As a result, the capacitance significantly decreases due to the desorption of water vapors from the pores of the MPG film. In fact, recovery time is defined as the time required for the sensor to recover from humidification, which is determined as 10% of the final relative humidity value.[42] Fig. 4(a) shows the resistance *versus* time behavior of the MPG humidity sensor, which shows a response/recovery time of 8/18 s. In Fig. 4(a), the decrease observed in sensor resistance with time can be attributed to the adsorption and condensation processes of water molecules on the sensing material as the relative humidity (RH) increases. Initially, water molecules are adsorbed onto the surface of the sensing material, occupying available adsorption sites. This process leads to

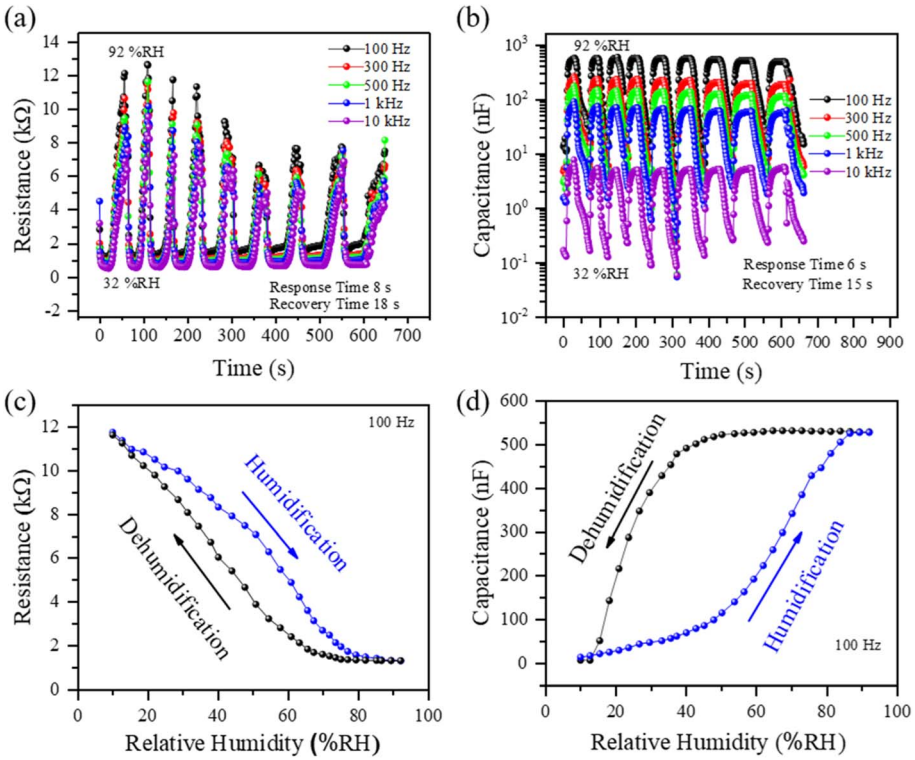

Fig. 4 Response and recovery times *versus* (a) resistance and (b) capacitance of MPG humidity sensor; hysteresis behavior of the fabricated MPG humidity sensor (c) resistance and (d) capacitance.

the polarization effect caused by dipole interactions between the adsorbed water molecules and the surface, momentarily increasing the resistance of the sensor. As RH continues to rise, the adsorption sites reach saturation, and additional water molecules form a multilayer structure through hydrogen bonding. This results in the formation of a condensed water film on the sensor surface. In this regime, ionic conduction becomes the dominant mechanism due to the mobility of hydronium ions (H_3O^+) within the water layer.[43] These ions facilitate charge transport through the condensed film, leading to a significant decrease in resistance over time. Moreover, during the initial duty cycles, the time-dependent reduction in resistance can also be explained by the gradual establishment of equilibrium between adsorption and ionic conduction processes. Once the adsorption sites are saturated, the system transitions to an ionic conduction-dominated regime, resulting in a continuous decrease in resistance across subsequent duty cycles.[24]

The capacitance *versus* adsorption and desorption properties of the MPG humidity sensor have also been tested at all five operating frequencies to observe the humidity response, as presented in Fig. 4(b). The outer layer of the composite thin film easily interacts with the water molecules during the sensing cycle. The MPG composite exhibits a good sensing response due to its hydrophilic nature and the uniformly spread water molecules on its surface. The recorded response/recovery time of the MPG sensor, in terms of capacitance *versus* time, is 6/15 s. The performance and efficiency of the fabricated humidity sensor at various frequencies show good repeatability and stability over time (Fig. S2). The sensor has been tested for several cycles at multiple frequencies, *i.e.*, 100 Hz, 300 Hz, 500 Hz, 1 kHz, and 10 kHz. The plot indicates that the MPG sensor is more sensitive and responsive at 100 Hz, but less sensitive at higher frequencies.

Hysteresis is one of the most important features that determines a lag between the adsorption and desorption of moisture detected by the sensing layer. For insight into the hysteretic behavior of the MPG ternary composite-based humidity sensor, the sensor was sequentially exposed to the adsorption process and then to the desorption process. The hysteresis response of the MPG composite with an incorporated humidity sensor at 100 Hz is shown in Fig. 4(c and d). The resistance *versus* relative humidity response exhibits low hysteresis, as shown in Fig. 4(c), compared to the capacitance *versus* relative humidity response in Fig. 4(d). The following equation calculates the hysteresis:

$$H = \pm \Delta H_{max}/2S \quad (3)$$

where ΔH_{max} is the divergence between the response of the humidity sensor for similar %RH values through adsorption and desorption operations, and S is the sensitivity. The values obtained from eqn (3) are 11.3% and 17.3% for resistive and capacitive responses, respectively. The comparison of both resistive and capacitive responses is presented in Table 1. The sensor exhibits good linearity and a fast response and recovery time.

Table 1 Resistance and capacitive responses of the MPG humidity sensor

Characteristics	Resistive	Capacitive
Sensitivity	135.8 Ω/%RH	11 nF/%RH
Response time	8 s	6 s
Recovery time	18 s	15 s
Hysteresis	11.3%	17.3%

3.4 Humidity sensing mechanism

Fig. 5(a) illustrates the general mechanism of humidity sensing. The MPG sensing layer's capacitance changes directly with the amount of adsorbed moisture. When exposed to humidity, hydroxyl groups from water molecules are adsorbed, forming a chemisorbed layer on the MPG layer. Subsequently, a physisorption process creates weakly bonded water molecule layers.[41] Increased humidity leads to the formation of successive physiosorbed layers, which enhances polarization and increases the capacitance of the active layer.[44]

The interplay between polyvinyl alcohol (PVA), methyl red (MR), and graphene oxide (GO) in the MPG blend for a humidity sensor represents a synergy of materials with complementary properties, specifically tailored for humidity sensing applications Fig. S3. All three materials play a key role in the MPG composite-based sensor. Due to hygroscopic properties and hydrophilic functional groups, which demonstrate a strong affinity for water, PVA was selected as a humidity-sensing polymer. PVA contains hydroxyl (OH) groups along its chain, making it highly responsive to changes in environmental humidity. When PVA adsorbs water vapor, the interaction between water molecules and the polymer alters its electrical properties, particularly its conductivity. As humidity increases, water vapor molecules are drawn to the PVA surface and form hydrogen bonds with the hydroxyl groups. However, PVA is inherently afflicted with intrinsic impedance, making it unsuitable for sensor use when used alone.[15] PVA stand-alone sensors have previously demonstrated low[45] and slow transient response time towards relative humidity.[46] To mitigate the impedance issue and improve the film's humidity sensitivity, it is crucial to combine PVA with another material. On the other hand, the main traits of GO are mainly large surface area, and hydroxyl groups attached to its surface. Another factor contributing to the increased sensitivity of GO is its highly rough surface, which leads to high porosity and facilitates the trapping of water molecules. When GO is used alone, it exhibits instability and lacks reproducibility, posing a significant challenge for sensor applications. When PVA is combined with GO, it creates more adsorption sites in the form of voids and defects, thereby enhancing the humidity-sensing properties. Additionally, GO serves as an anchor to improve electron transport, thereby modifying the properties of PVA. When the sensor is

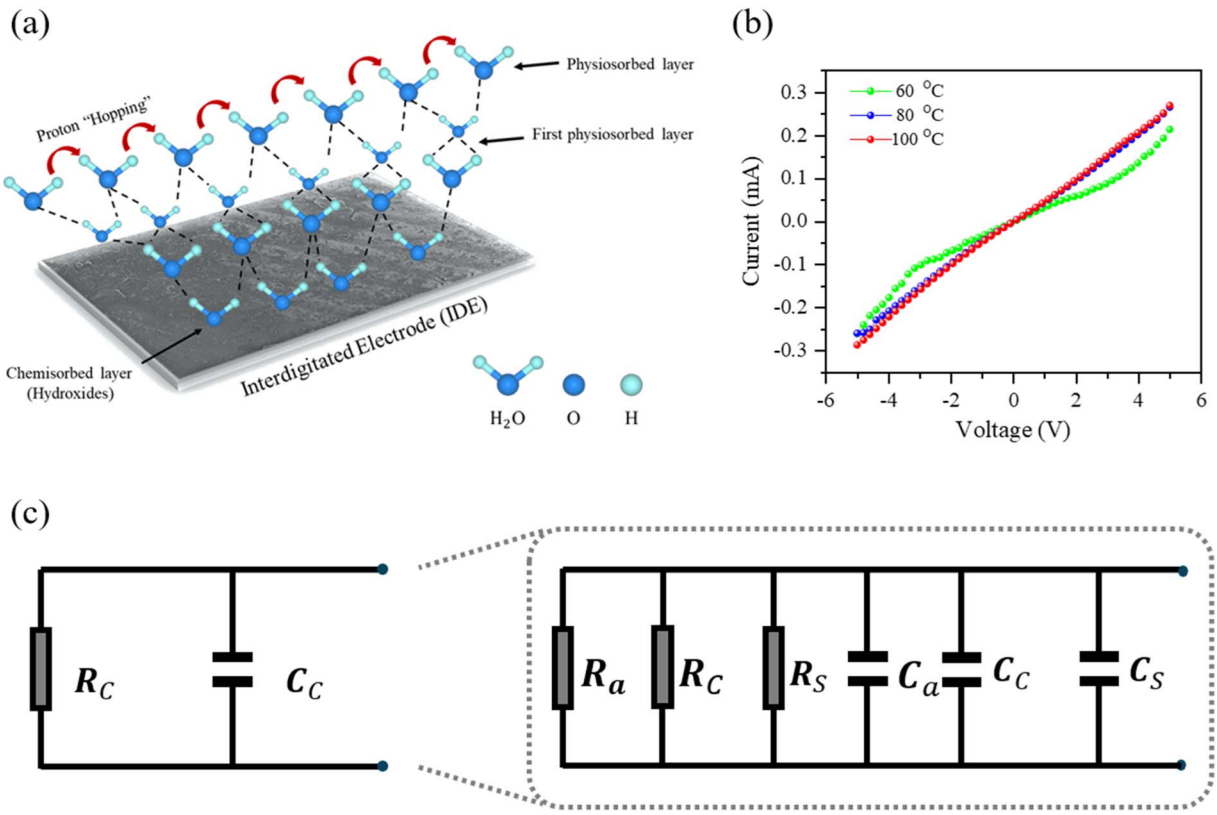

Fig. 5 (a) Sensing mechanism of the MPG composite-based humidity sensor, (b) temperature dependent *I*–*V* characteristics of the MPG sensor measured at (a) 60 °C, (b) 80 °C, and (c) 100 °C, detailed and simplified schematic diagrams of the electrical equivalent circuit representing the MPG humidity sensor.

exposed to varying humidity levels, it readily interacts with water vapor, resulting in fluctuations in the dielectric constant. As humidity increases, the hydrogen bonding between water vapor and the hydroxyl (OH) groups in PVA and GO becomes stronger. This leads to a higher concentration of H^+ ions, which can hop between water vapor molecules *via* the Grotthuss mechanism. With an increase in water vapor in the atmosphere, more H^+ ions can migrate, resulting in a higher conductivity of the PVA:GO material.[8]

Methyl red is a non-conductive material that does not support the flow of electronic current under normal circumstances. However, when it is exposed to a humid environment, its dielectric constant changes due to the physisorption phenomenon where a large number of water molecules are adsorbed, causing changes in capacitance. These changes in capacitance depend upon polarization. The increased adsorption of water molecules in the thin film leads to a rise in capacitance due to an effective increase in the dielectric permittivity of methyl red.

The resistance of the MPG sensor exhibits a linear decrease with increasing humidity levels across the entire humidity range of 32–92% RH. The sharp reduction in resistance, even at lower humidity levels, can be attributed to the presence of GO, which possesses a highly porous surface suitable for trapping water molecules. GO surface chemisorbs and physisorbs water molecules into their active sites through hydrogen bonding. Since MR is not a conducting material, low levels of relative humidity (RH) have minimal impact on the overall impedance of the sensor. However, at higher relative humidity (RH) levels, the capacitance changes due to the physisorption of water molecules, resulting in a notable change in the resistance of the MPG sensor. Owing to the properties of all three moieties in the ternary composite-based MPG sensor is explored both as a capacitive and resistive sensor in the present work.

The MPG sensor's performance depends on the material's porosity; more pores lead to more significant water adsorption. The water molecules interact with MR and PVA and fill GO pores, changing MPG's dielectric constant. The capacitance increase in humidity sensors results from the interaction between the sensing material and water molecules, altering the dielectric properties. This can be correlated to the parallel plate capacitor eqn (4).

$$C = \varepsilon \times A/d \tag{4}$$

where C is capacitance, ε is permittivity, A is the area and d is a gap between plates.

Chemisorbed and initial physisorbed water layers have tightly bonded double bonds, whereas successive physisorbed layers contain loosely bonded single hydrogen ions, which introduce changes in dielectric permittivity and increase capacitance.[42] Water's high permittivity leads to polarization, creating dipoles within the active layer that align with an electric field, thereby increasing capacitance. Water also creates trap states and recombination centers, leading to charge trapping and recombination, especially at low frequencies. Additionally, water spreads to boundaries between layers, producing interfacial dipoles and increased interfacial capacitance. The significant increase in MPG composite permittivity upon water adsorption enhances the film's capacitance. The relationship between dielectric permittivity and capacitance is given by eqn (5).

$$\frac{C_s}{C_o} = \left(\frac{\varepsilon_w}{\varepsilon_d}\right)^n \tag{5}$$

where C_s and C_o are saturated and initial capacitances, respectively, while ε_w and ε_d are dielectric permittivities in wet and dry conditions, respectively, and n is the morphological factor. Now, when the permittivity of the MPG composite drastically increases upon adsorption of moisture content on its surface, the capacitance of the composite film inevitably enhances. The rise in capacitance with increasing relative humidity can also be explained by considering different polarizabilities. Polarizability is correlated to the polarization eqn (6), which provides information about the state of the dielectric and, in turn, the capacitance of the material.

$$P = N\alpha E \tag{6}$$

where P is the polarization, α is the polarizability, and E is the electric field. Several sources of polarizability affect the capacitance of dielectric materials: electronic polarizability (displacement of electron cloud), ionic polarizability (change in distance between ions), and dipolar polarizability (orientation of dipoles). Although electronic polarization has a minimal impact, ionic and dipolar polarizations have a significant influence on the MPG composite. Ionic polarization occurs due to internal charge transfer complexes, while dipolar polarization arises from dipoles in adsorbed water molecules, which is crucial for a capacitive-humidity response.

When the MPG sensor's active layer adsorbs moisture, ionic functional groups dissociate, increasing conductivity and reducing sensor resistance. PVA and MR, with high adsorption capacities, attract water molecules, decreasing MR's resistance and, consequently, the sensor's overall resistance. MR also fills voids in GO, ensuring continuous pathways. The strong interplay among PVA, MR, and GO enhances the sensor's sensitivity to humidity, making it highly responsive.[47]

The composite film has been tested over a voltage range of −5 to 5 V at various temperatures. Fig. 5(b) shows that the electrical properties of the thin film can be altered by changing the temperature. It can be observed that as the temperature increases, the conductivity of the thin film increases, thereby enhancing the current flow. This effect can be attributed to the large number of electrons available due to the vibration of the atomic lattice, which ultimately influences the free path of electrons in the film. For the design and optimization of electronic devices, it is very crucial to study the effect of the temperature at which the device is expected to operate.

The detailed and simplified equivalent circuit diagrams of the MPG humidity sensor are shown in Fig. 5(c), respectively. The circuit includes a capacitor representing polarization and a resistor depicting various conducting species. Three types of dielectrics exist due to air, the composite material, and the

Table 2 Benchmarking MPG against reported MR, PVA, and GO sensors

Ternary composite sensing layer	Humidity sensing range (%RH)	Sensitivity	Response time (s)	Recovery time (s)	Ref.
Methyl red	30–95	0.02 (nF/%RH)	10	10	48
Polyvinyl alcohol	32–92	48 (pF/%RH)	103.27	13	49
Graphene oxide	40–99	~32, 146% at 100 Hz	174	40	50
Methyl green	40–80	122.37 (pF/%RH)	200	60	35
GO/PEDOT: PSS	—	1220 (pF/%RH)	—	—	51
Graphene oxide/Polyvinyl alcohol	40–80	—	—	—	52
Graphene/Methyl red	35–100	2.3 pF to 66 nF at %RH (5–100)	0.251	0.35	10
MR/PVA/GO (MPG)	32–92	11 (nF/%RH)	6	15	Present work

silver substrate, producing three capacitances and resistances: C_a, C_c, C_s, R_a, R_c, and R_s. The dielectric of air within the pore area corresponds to R_a and C_a. The capacitance and resistance of the composite, C_c, and R_c, reflect the dielectric properties of the active layer. R_s and C_s arise from the silver substrate's dielectric. Typically, the dielectric permittivity of the MPG composite is much higher than that of the substrate and air. Additionally, the gap between the plates of C_a and C_s is more significant than that of C_c, making $C_c >> C_a$ and C_s. Therefore, only C_c is considered, while C_a and C_s are neglected. Similarly, R_c is considered lower, assuming R_a*and* $R_s > R_c$, resulting in the simplified circuit in Fig. 5(c). Table 2 compares the sensing parameters (sensing range, sensitivity, response/recovery times) of the MPG humidity sensor with other stand-alone reported sensors. The results indicate that our proposed sensor exhibits exceptional performance, particularly in terms of high sensitivity and fast response, likely due to the presence of methyl red.

4 Conclusion

A novel ternary composite humidity sensor based on methyl red (MR), polyvinyl alcohol (PVA), and graphene oxide (GO) was successfully fabricated and demonstrated promising performance. The unique dielectric, morphological, and conductive properties of the selected materials, combined with their cost-effectiveness and availability, contributed to the sensor's efficiency. The sensor operates as a dual-mode device, capable of detecting both capacitive and resistive humidity within the relative humidity range of 32–92% RH. It exhibits rapid response and recovery times, measured at 6/15 seconds for the capacitive mode and 8/18 seconds for the resistive mode, respectively. The capacitive sensitivity was notably high, achieving 11 nF/%RH at 100 Hz. Additionally, the sensor's performance was evaluated across various frequencies (100 Hz, 300 Hz, 500 Hz, 1 kHz, and 10 kHz), providing a comprehensive understanding of both its capacitive and resistive behavior. The facile spin casting approach and subsequent thermal annealing at 100 °C enabled the development of an enhanced porous structure, further improving the device's sensitivity. Given its cost-effectiveness, rapid response, and broad sensing range, this ternary composite humidity sensor has significant potential for integration into hygrometers and real-time relative humidity monitoring systems for electronic applications.

Ethical statement

The human respiration/breath-related measurements carried out in this study were performed with the informed consent of the volunteers(s). All procedures were non-invasive, no personally identifiable information was collected, and the experiments compiled with ethical standards for research involving human participants.

Author contributions

Mushahid Hussain: conceptualization, visualization, investigation, methodology, formal analysis, investigation, writing – original draft, writing – review & editing. Nadir Ali Khan: supervision, writing, review & editing. Wei-Chun Lin: supervision, investigation, validation, writing – review & editing. Muhammad Yaseen: investigation, writing – review & editing, DAta curation. Fakhra Aziz: investigation, methodology, formal analysis, investigation, writing – review & editing. Muhammad Ali: visualization and validation, Naseem Abbas: formal analysis, investigation, writing – review & editing.

Conflicts of interest

The authors declare no competing financial interests.

Data availability

All data supporting the findings of this study are provided in the supplementary information (SI). Supplementary information is available. See DOI: https://doi.org/10.1039/d5ra07420g.

Acknowledgements

The authors acknowledge the University of Peshawar, Peshawar, Pakistan; National Sun Yat-sen University, Kaohsiung, Taiwan; and Sejong University, Korea, for providing access to state-of-the-art equipment for the investigation of sensors and thin films. The authors are also grateful to the University of Education, Lahore, Pakistan, for providing partial support through the Pakistan Science Foundation research grant [PSF/Res/P-EU/Chem 612, 2022].

References

1 R. Akram, *et al.*, Capacitive and conductometric type dual-mode relative humidity sensor based on 5, 10, 15, 20-tetra phenyl porphyrinato nickel (II)(TPPNi), *Polymers*, 2021, **13**(19), 3336.
2 M. Saleem, *et al.*, Synthesis and application of Ni (II) 5, 10, 15, 20-tetrakis (4′-isopropylphenyl) porphyrin in a surface-type multifunctional sensor, *Phys. Scr.*, 2010, **82**(1), 015703.
3 T. Q. Trung, *et al.*, Transparent, stretchable, and rapid-response humidity sensor for body-attachable wearable electronics, *Nano Res.*, 2017, **10**(6), 2021–2033.
4 M. I. Azmer, *et al.*, Compositional engineering of VOPcPhO-TiO2 nano-composite to reduce the absolute threshold value of humidity sensors, *Talanta*, 2017, **174**, 279–284.
5 R. Akram, *et al.*, Integrated capacitive-and resistive-type bimodal relative humidity sensor based on 5, 10, 15, 20-tetraphenylporphyrinatonickel (II)(TPPNi) and zinc oxide (ZnO) nanocomposite, *ACS Omega*, 2022, **7**(34), 30590–30600.
6 M. Yaseen, *et al.*, Green synthesis, structural tailoring, and optical optimization of porphyrins for high-performance thin film resistive-capacitive sensors, *J. Mol. Struct.*, 2025, **1335**, 141985.
7 M. Yaseen, *et al.*, Synthesis and investigation of linear and nonlinear optical properties of an octahedral metalloporphyrin, *Opt. Mater.*, 2024, **149**, 115092.
8 S. A. Rahman, *et al.*, Highly sensitive and stable humidity sensor based on the bi-layered PVA/graphene flower composite film, *Nanomaterials*, 2022, **12**(6), 1026.
9 Y. Li, *et al.*, Poly (4-vinylpyridine)/carbon black composite as a humidity sensor, *Sens. Actuators, B*, 2007, **123**(1), 554–559.
10 S. Ali, *et al.*, All-printed humidity sensor based on graphene/methyl-red composite with high sensitivity, *Carbon*, 2016, **105**, 23–32.
11 C.-C. Yang, S.-J. Lin and G.-M. Wu, Study of ionic transport properties of alkaline poly (vinyl) alcohol-based polymer electrolytes, *Mater. Chem. Phys.*, 2005, **92**(1), 251–255.
12 J. S. Park, J. W. Park and E. Ruckenstein, A dynamic mechanical and thermal analysis of unplasticized and plasticized poly (vinyl alcohol)/methylcellulose blends, *J. Appl. Polym. Sci. Appl. Polym. Symp.*, 2001, **80**(10), 1825–1834.
13 M. Edwards Sr, *et al.*, Determining the electrical mechanism of the surface resistivity property of doped polyvinyl alcohol (PVA) and the pyroelectric property of polyvinylidene difluoride (PVDF) thin films. in *Infrared Sensors, Devices, and Applications V*. 2015. SPIE.
14 M.-R. Yang and K.-S. Chen, Humidity sensors using polyvinyl alcohol mixed with electrolytes, *Sens. Actuators, B*, 1998, **49**(3), 240–247.
15 B. Deshkulkarni, *et al.*, Humidity sensing using polyaniline/polyvinyl alcohol nanocomposite blend. in *IOP Conference Series: Materials Science and Engineering*. IOP Publishing. 2018.
16 A. Sun, L. Huang and Y. Li, Study on humidity sensing property based on TiO2 porous film and polystyrene sulfonic sodium, *Sens. Actuators, B*, 2009, **139**(2), 543–547.
17 Y. Li, M. Yang and Y. She, Humidity sensitive properties of crosslinked and quaternized poly (4-vinylpyridine-co-butyl methacrylate), *Sens. Actuators, B*, 2005, **107**(1), 252–257.
18 M. Gaur, *et al.*, Biomedical applications of carbon nanomaterials: fullerenes, quantum dots, nanotubes, nanofibers, and graphene, *Materials*, 2021, **14**(20), 5978.
19 A. N. Banerjee, Graphene and its derivatives as biomedical materials: Future prospects and challenges, *Interface Focus*, 2018, **8**(3), 20170056.
20 J. Feng, *et al.*, Fabrication and evaluation of a graphene oxide-based capacitive humidity sensor, *Sensors*, 2016, **16**(3), 314.
21 Z. Ahmad, *et al.*, Humidity-dependent characteristics of methyl-red thin film-based Ag/methyl-red/Ag surface-type cell, *Phys. E Low-dimens. Syst. Nanostruct.*, 2008, **41**(1), 18–22.
22 W. Yuan and G. Shi, Graphene-based gas sensors, *J. Mater. Chem. A*, 2013, **1**(35), 10078–10091.
23 G. Hassan, M. Sajid and C. Choi, Highly sensitive and full range detectable humidity sensor using PEDOT: PSS, methyl red and graphene oxide materials, *Sci. Rep.*, 2019, **9**(1), 15227.
24 R. Liang, *et al.*, Research progress of graphene-based flexible humidity sensor, *Sensors*, 2020, **20**(19), 5601.
25 X. Song, *et al.*, Tunable negative permittivity in graphene/poly (vinylidene fluoride) composites with low percolation threshold, *Adv. Eng. Mater.*, 2024, **26**(2), 2300203.
26 Y. Seekaew and C. Wongchoosuk, A novel graphene-based electroluminescent gas sensor for carbon dioxide detection, *Appl. Surf. Sci.*, 2019, **479**, 525–531.
27 D. Hernández-Rivera, *et al.*, A capacitive humidity sensor based on an electrospun PVDF/graphene membrane, *Sensors*, 2017, **17**(5), 1009.
28 K. Gul, *et al.*, Synthesis and characterization of graphene/Fe3O4 nanocomposite as an effective adsorbent for removal of acid red-17 and remazol brilliant blue R from aqueous solutions, *Curr. Nanosci.*, 2016, **12**(5), 554–563.
29 R. Yuan, *et al.*, Efficient synthesis of graphene oxide and the mechanisms of oxidation and exfoliation, *Appl. Surf. Sci.*, 2017, **416**, 868–877.
30 M. Hussain, *et al.*, Design and fabrication of a fast response resistive-type humidity sensor using polypyrrole (ppy) polymer thin film structures, *Polymers*, 2021, **13**(18), 3019.
31 D. Liu, *et al.*, Effect of annealing on phase structure and mechanical behaviors of polypropylene hard elastic films, *J. Polym. Res.*, 2013, **20**(5), 126.
32 C. W. Chen, *et al.*, Development of moisture-absorbing and antioxidant active packaging film based on poly (vinyl alcohol) incorporated with green tea extract and its effect on the quality of dried eel, *J. Food Process. Preserv.*, 2018, **42**(1), e13374.
33 S. Ishaq, *et al.*, Dielectric and impedance spectroscopic studies of three phase graphene/titania/poly (vinyl alcohol) nanocomposite films, *Results Phys.*, 2018, **11**, 540–548.
34 K. A. Sariningsih, I. Rostini and K. Haetami, Methyl red indicator on smart packaging as a freshness sensor for tilapia fillets, *Asian Food Sci. J*, 2019, **13**(4), 1–9.

35 U. Afzal, *et al.*, Fabrication of a surface type humidity sensor based on methyl green thin film, with the analysis of capacitance and resistance through neutrosophic statistics, *RSC Adv.*, 2021, **11**(61), 38674–38682.
36 A. D. Smith, *et al.*, Resistive graphene humidity sensors with rapid and direct electrical readout, *Nanoscale*, 2015, **7**(45), 19099–19109.
37 Y. Zhang, *et al.*, Design and fabrication of a novel humidity sensor based on ionic covalent organic framework, *Sens. Actuators, B*, 2020, **324**, 128733.
38 M. R. Mahboob, Z. H. Zargar and T. Islam, A sensitive and highly linear capacitive thin film sensor for trace moisture measurement in gases, *Sens. Actuators, B*, 2016, **228**, 658–664.
39 Y. Zhang, *et al.*, Characterization and humidity sensing properties of the sensor based on Na2Ti3O7 nanotubes, *J. Nanosci. Nanotechnol.*, 2014, **14**(6), 4303–4307.
40 A. Tripathy, *et al.*, Role of morphological structure, doping, and coating of different materials in the sensing characteristics of humidity sensors, *Sensors*, 2014, **14**(9), 16343–16422.
41 A. G. Al-Sehemi, *et al.*, Sensing performance optimization by tuning surface morphology of organic (D-π-A) dye based humidity sensor, *Sens. Actuators, B*, 2016, **231**, 30–37.
42 M. Arafat, *et al.*, Gas sensors based on one dimensional nanostructured metal-oxides: a review, *Sensors*, 2012, **12**(6), 7207–7258.
43 T. Fei, *et al.*, Polymeric humidity sensors with nonlinear response: Properties and mechanism investigation, *J. Appl. Polym. Sci.*, 2013, **130**(3), 2056–2061.
44 G. Paterakis, *et al.*, Highly sensitive and ultra-responsive humidity sensors based on graphene oxide active layers and high surface area laser-induced graphene electrodes, *Nanomaterials*, 2022, **12**(15), 2684.
45 E. M. Amin, N. C. Karmakar and B. Winther-Jensen, Polyvinyl-alcohol (PVA)-based RF humidity sensor in microwave frequency, *Prog. Electromagn. Res. B*, 2013, **54**, 149–166.
46 Z.-C. Chen, *et al.*, Application of self-heating graphene reinforced polyvinyl alcohol nanowires to high-sensitivity humidity detection, *Sens. Actuators, B*, 2021, **327**, 128934.
47 F. Yavari and N. Koratkar, Graphene-based chemical sensors, *J. Phys. Chem. Lett.*, 2012, **3**(13), 1746–1753.
48 Z. Ahmad, *et al.*, Humidity-dependent characteristics of methyl-red thin film-based Ag/methyl-red/Ag surface-type cell, *Phys. Rev. E*, 2008, **41**(1), 18–22.
49 H. U. Rashid, The synthesis and fabrication of polyvinyl alcohol nanofibers based capacitive relative humidity sensor, *Sir Syed University Research Journal of Engineering & Technology*, 2021, **11**(01), 31–35.
50 Z. Song, *et al.*, High-sensitivity paper-based capacitive humidity sensors for respiratory monitoring, *IEEE Sens. J.*, 2022, **23**(3), 2291–2302.
51 F. J. Romero, *et al.*, Fabrication and characterization of humidity sensors based on graphene oxide–PEDOT: PSS composites on a flexible substrate, *Micromachines*, 2020, **11**(2), 148.
52 Z. Cui, *et al.*, A Highly Responsive Graphene Oxide Humidity Sensor Based on PVA Nanofibers, *Langmuir*, 2024, **40**(31), 16361–16366.